

## Simulation of Seismic Wave Propagation in a Deep Mine

*Ramin Saleh, Bernd Milkereit, Qinya Liu*  
 Department of Physics, University of Toronto

### Summary

Understanding the propagation of seismic waves in deep mines in a presence of very strong elastic contrasts, such as topography, tunnels and ore-bodies is still a challenge. For engineering purposes, amplitudes and travel times of seismic events are critical parameters that have to be determined at various locations in a mine. These parameters are useful in preparing risk maps or to better understand the process of spatial and temporal stress distributions in a mine. Simple constant velocity models used for mine monitoring, cannot explain the observed complexities in scattered seismic waves. In hard-rock environments modeling of elastic seismic wavefield require detailed 3D petrophysical, infrastructure and topographical data to simulate the propagation of seismic wave with a frequencies up to few kilohertz. In this study, the effects of strong elastic contrasts on the propagation of seismic waves will be illustrated using 2D/3D finite difference method.

### Introduction

Most of the physical properties of crystalline rock are highly stress dependent. As such, the nonlinear and anisotropic variability of the in situ P- and S-wave velocities can potentially be linked directly to changes in the stress field. Canadian underground mines are some of the deepest mines in the world, and they are mostly located in Sudbury, Ontario. Highly stressed Sudbury mining camp offers an interesting setting for fundamental research in to time-lapse monitoring of seismicity, stress, and stress dependent physical properties at deep mines. In an active underground mine site, controlled production blasts and microseismic monitoring are conventionally the main tools to better understand the process of rock fracturing and rock deformation. The presence of very strong elastic contrasts, such as massive orebodies, tunnels, stopes and infrastructure have a significant impact on the propagation of seismic waves. Since the complexity of seismic wave propagation can affect the distribution of energy significantly, the use of a more accurate model is required to predict the ground motion. For example, the conventional empirical method used to calculate peak particle velocities and accelerations (PPVs/PPAs), tends to underestimate the intensity of seismic waves in stopes or areas close to blast sites, which could be corrected if a more realistic model was implemented.

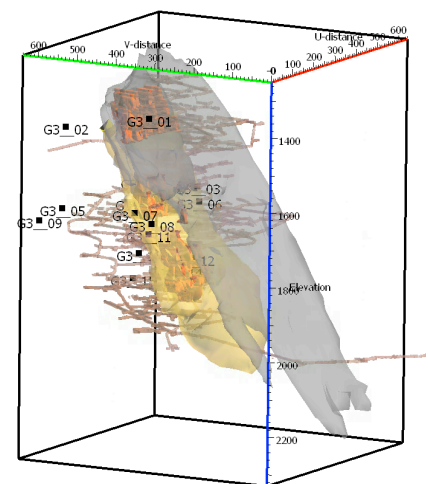


Figure 1. Geological 3D used mine model including ore bodies (yellow and grey), tunnels (brown) and stopes (red). Black cubes show 3D distribution of 3C geophones at the mine.

## Method

With the recent availability of detailed 3D rock property models of mines, in addition to the development of efficient numerical techniques and parallel computation facilities, a solution for the propagation of seismic waves at the mine size level is achievable. In order to model the effects of high elastic contrasts on the propagation of seismic waves within a 3D underground mine, a full elastic/viscoelastic finite difference time domain modeling package is used [Bohlen, 2002].

## Results

**2D modeling:** To visualize the possible effects of available elastic contrasts, a vertical 2D section from a 3D detailed petrophysics model, Figure 1, is extracted and used. The used 2D section is 400 m x 600 m in x and z direction respectively. For the simulation, Ricker wavelet signal with a central frequency of 200Hz was used as source function. The model is discretized into structured grids with the grid cell size of 0.1 m. The cell size is chosen based on the selected source central frequency and FD stability criteria for each simulation.

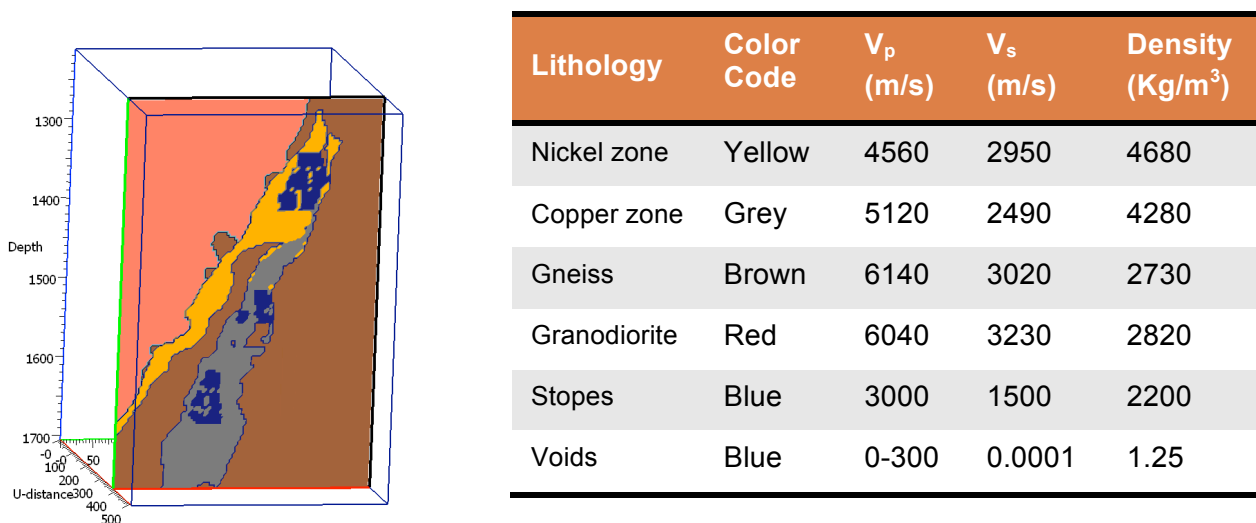


Figure 2. On the left, a petrophysical 2D section of an underground mine model is shown. The mine is located in Sudbury Ontario, Canada. The model shows geology in addition to designed stopes at the mine. On the right, table illustrates the elastic properties of all contrasts used in 2D/3D models. Note that after production blasts, crashed orebodies in stopes will be mined out and a void will be remained. However remained voids will be backfilled with cement after a while. Thus the blue areas in the table could represent both void/cement in this study.

In this part, the goal is to understand the effects of mining process on the propagation of seismic waves in a stope areas, therefore the same source property and the same petrophysical model geometry is used for all simulation. Depends on mine state of production, the orebodies located inside the stopes could be intact, mine out or backfilled with cement. Each of these scenarios is being studied here and the results are illustrated in Figures 3, 4 and 5 respectively. In general, modelling results show the complexity of the propagating waves in mine environments. In Figure 3, the propagated waves do not show significant changes in amplitude and orebody mostly impacted travel time values. However, strong scattering effect and P to S-wave conversion can be observed especially for higher frequencies.

Results in both Figure 4 and 5, show strong reflections of P-waves from stope areas, though this effect is more dominant where voids are exist. Such a strong reflection at the mine leads to presence of shadow zone in front of those contrasts. Also note the change of polarity for reflected seismic waves from stope areas. The change of polarity due to these reflections imposes a caution for source mechanism studies.

The cemented backfill region, a low velocity region, has trapped the energy and this effect is more dominant for S-waves. Also this region is mainly in charge of changes in travel time with as mining progress, and clearly shows the need for updating the used velocity model at a mine.

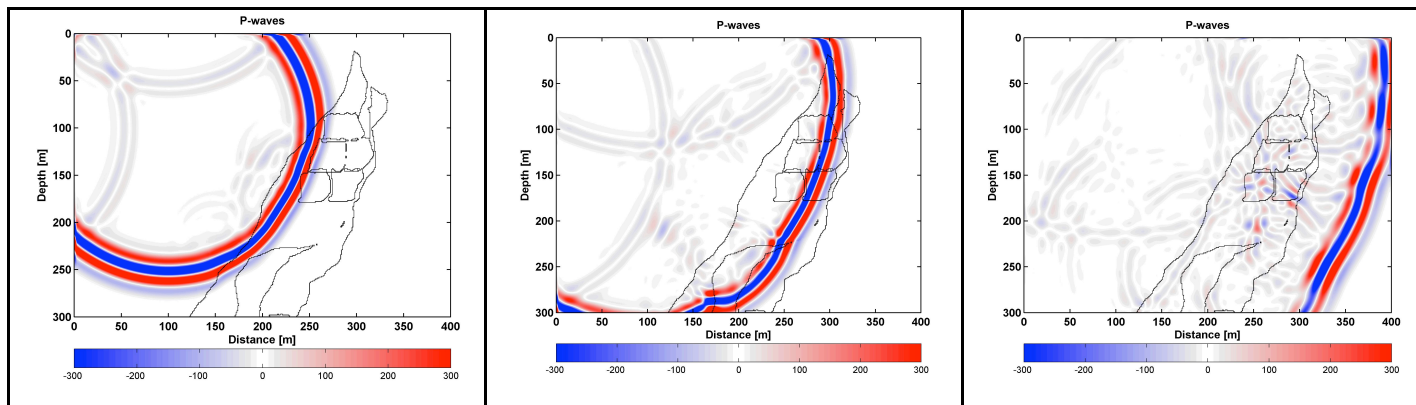


Figure 3. P-wave snapshots here represent a 2D simulation of a blast located on the top left corner of model, as if there is no mining activity in stope areas. The used source central frequency is 200 Hz.

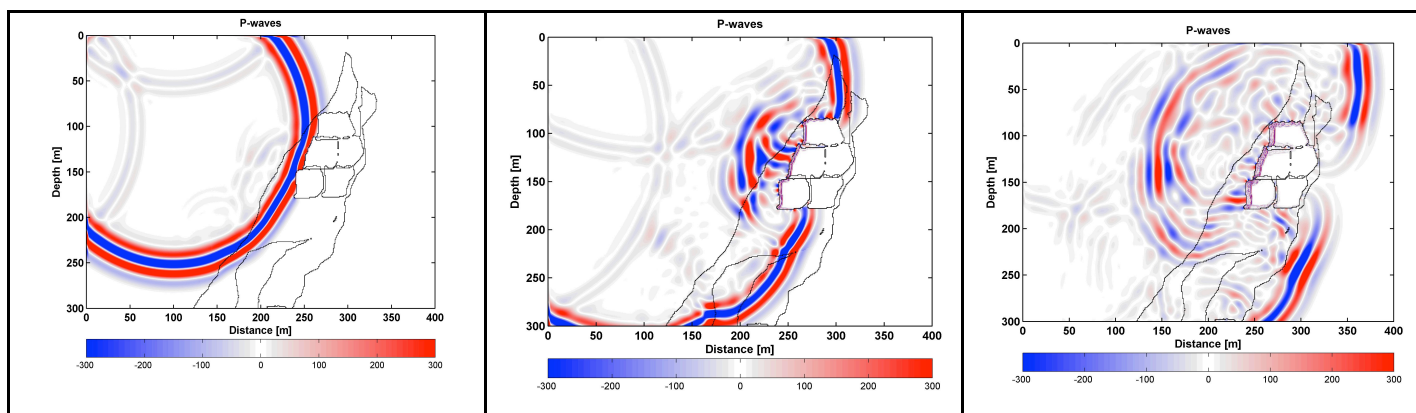


Figure 4. The used model represents a mine where orebodies are mined out and the voids remained in stope areas, where you see strong reflections. The same source is used here.

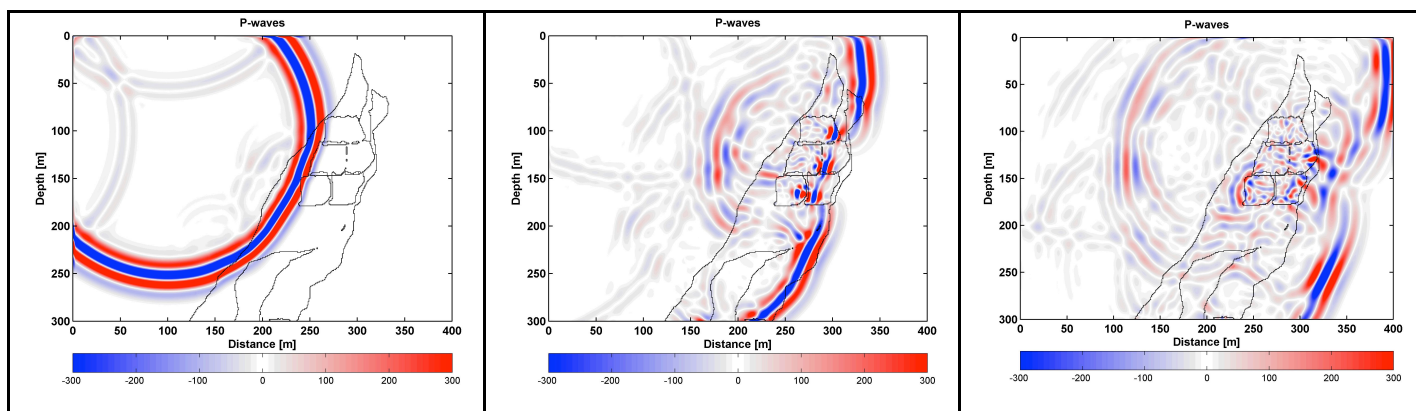


Figure 5. Snapshots represent a mine model after orebodies are mined out and voids cemented backfilled. Backfilled areas are very low velocity contrast, which results in strong reflection and significant travel time changes.

### 3D modelling:

In this part the effect of using a full 3D variable velocity model on the estimated travel time of propagated seismic waves, in comparison to constant velocity model is studied. The need for updating the velocity model for active mines, where mine is evolving over time, has been shown. Results in Figure 7 shows the variation of estimated travel time of 3D variable velocity model from constant velocity model. Depends on the geometries of receivers and sources in respect to each other and orebodies, estimated travel times shows significant variation compare to the ones estimated from constant velocity model.

Geophone	Distance to blast	North (m)	Easting (m)	Depth (m)
G02	151 m	148.3	135.7	358.1
G04	153 m	366.3	286.7	277.1
G01	193 m	196.3	107.7	170.1
G10	205 m	388.3	341.7	302.1
G03	239 m	371.3	285.7	139.1
G07	256 m	152.3	315.7	181.1
G05	261 m	78.3	307.7	327.1
G06	262 m	344.3	313.7	120.1
G13	290 m	324.3	441.7	263.1
G09	290 m	73.3	339.7	383.1
G11	313 m	140.3	357.7	138.1
G08	327 m	112.3	328.7	114.1
G15	342 m	339.3	497.7	286.1
G12	345 m	324.3	439.7	126.1
G14	357 m	304.3	467.7	145.1

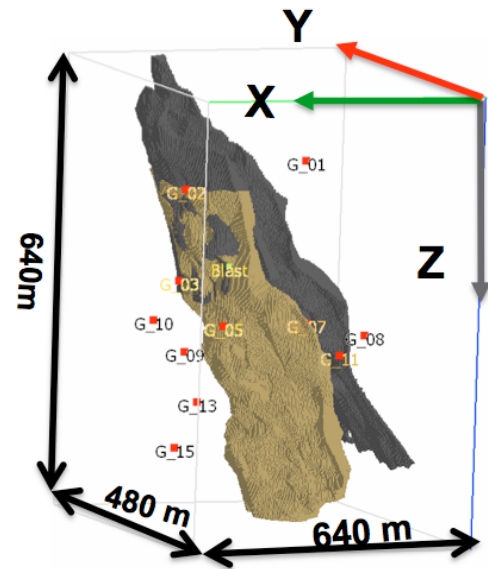


Figure 6. On the left, table of geometry of 3-C geophones installed in the Sudbury deep mine. On the right, the used 3D detailed petrophysical model of an underground mine. Seismic arrays are illustrated with red cubes and location of used blast is shown in yellow.

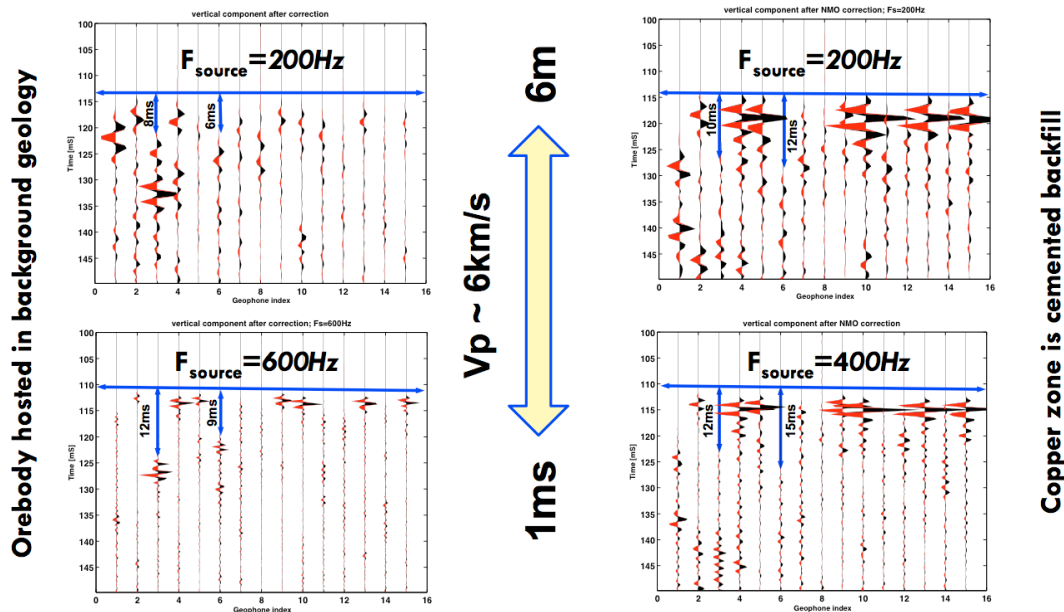


Figure 7. Synthetic trace's travel time are corrected based on distance between each geophone to blast using a constant velocity value of 6 Km/s. Based on the location of geophones in respect to the blast and orebody, some traces are almost flat and some others are up to 10-15 ms off from flat correction line. Such a travel time difference in a hardrock environment will translate to spatial difference of 60-90m. Depending on the used algorithm for events location, such a travel time difference could introduce a considerable error into location scheme.

## Conclusions

A homogeneous velocity background model is inaccurate in deep mines due to the presence of very strong elastic contrasts. This very heterogeneous medium results in a complexity of wave propagation with variations in amplitude, travel time, and phase. The significance of these effects strongly depends on the size, shape, petrophysical properties and the frequency content of seismic source. The modelling results verify the amplification effects at regions with high  $V_p/V_s$  ratio. Presence of cement or void in models, showed changes in polarity and/or creation of shadow zones. The observed complexity of the wave propagation suggests the necessity for further consideration of such effects in the determination of focal mechanisms and full moment tensor inversions.



## Acknowledgements

The project was funded as a SUMIT ORF project coordinated by CEMI and NSERC. We would like to thank Vale Ltd and Glencore for providing us with data and access to their mine properties.

## References

- Bohlen, T., 2002, Parallel 3-D viscoelastic finite difference seismic modeling: Computers and Geosciences, 28 (8), 887-889.
- Duff, D.J., valley, B., Milkereit, B., and McGauhey, J., , Rock Mass Response to Deep Mining Induced Stress –addressing the geomechanical needs. Proceeding of the Australian Center for Geomechanic, 9p, 2011.
- Gharti, H. N., V. Oye, and M. Roth, 2008, Traveltimes and waveforms of microseismic data in heterogeneous media: 78th Annual International Meeting, SEG, Expanded Abstracts, SEG, 27.
- Robertsson, J. O., 1996, a numerical free-surface condition for elastic/viscoelastic finite-difference modelling in the presence of topography, Geophysics, 61(6), 1921–1934.